Membrane-associated farnesylated UCH-L1 promotes α-synuclein neurotoxicity and is a therapeutic target for Parkinson's disease

Zhihua Liu[a,b], Robin K. Meray[a,b], Tom N. Grammatopoulos[b], Ross A. Fredenburg[b], Mark R. Cookson[c], Yichin Liu[a], Todd Logan[b], and Peter T. Lansbury, Jr.[a,b,1]

[a]Center for Neurologic Diseases, Brigham and Women's Hospital and Department of Neurology, Harvard Medical School, 65 Landsdowne Street, Cambridge, MA 02139; [b]Link Medicine Corporation, 161 First Street, Cambridge, MA 02142; and [c]Laboratory of Neurogenetics, National Institutes of Health, Building 35, 9000 Rockville Pike, Bethesda, MD 20892

Edited by David M. Holtzman, Washington University School of Medicine, St. Louis, MO, and accepted by the Editorial Board January 1, 2009 (received for review July 14, 2008)

Ubiquitin C-terminal hydrolase-L1 (UCH-L1) is linked to Parkinson's disease (PD) and memory and is selectively expressed in neurons at high levels. Its expression pattern suggests a function distinct from that of its widely expressed homolog UCH-L3. We report here that, in contrast to UCH-L3, UCH-L1 exists in a membrane-associated form (UCH-L1^{M}) in addition to the commonly studied soluble form. C-terminal farnesylation promotes the association of UCH-L1 with cellular membranes, including the endoplasmic reticulum. The amount of UCH-L1^{M} in transfected cells is shown to correlate with the intracellular level of α-synuclein, a protein whose accumulation is associated with neurotoxicity and the development of PD. Reduction of UCH-L1^{M} in cell culture models of α-synuclein toxicity by treatment with a farnesyltransferase inhibitor (FTI-277) reduces α-synuclein levels and increases cell viability. Proteasome function is not affected by UCH-L1^{M}, suggesting that it may negatively regulate the lysosomal degradation of α-synuclein. Therefore, inhibition of UCH-L1 farnesylation may be a therapeutic strategy for slowing the progression of PD and related synucleinopathies.

farnesylation | synuclein

Ubiquitin C-terminal hydrolase-L1 (UCH-L1) is a 223-amino acid protein whose expression is limited to few tissues, including brain, testes (1), ovaries (2), and certain peripheral tumors (3–5). UCH-L1 is robustly expressed in neurons, comprising 1–2% of total brain protein (6), and its absence in mice due to spontaneous intragenic deletions produces neurologic and neurodegenerative phenotypes (1, 7). An S18Y polymorphism in UCH-L1 reduces susceptibility to Parkinson's disease (PD) (8–12) and Alzheimer's disease (AD) (13) and may influence the age at onset of Huntington's disease (14). A recent study suggests that the S18Y substitution may confer antioxidant function to UCH-L1 (15). The genetic association between UCH-L1 and AD is consistent with findings that transduction of soluble UCH-L1 protein into hippocampal slices treated with amyloid beta (Aβ) restores synaptic function, and that transduction of UCH-L1 into a mouse model of AD rescues contextual memory deficits (16). Expression of UCH-L1 in the brain is abnormally low in lysosomal storage diseases (17) and in diffuse Lewy body disease (18), but it is unknown whether low levels of UCH-L1 predispose to disease or are a response to the pathogenic process.

Although the weak hydrolytic activity and substrate specificity of UCH-L1 (19) suggest a role in the proteasome-dependent protein degradation pathway, its true in vivo role remains unclear. Indeed, recent studies have indicated that UCH-L1 does not significantly influence activity of the ubiquitin-proteasome system (7, 15). The study reported here was initiated to identify posttranslational modifications of UCH-L1 that distinguish it from its widely expressed homolog UCH-L3 and that may be critical for its in vivo activity. UCH-L1 is *O*-glycosylated (20) and monoubiquitinated (21). We report here an additional modification that may significantly have an impact on its enzymatic and/or binding activities: UCH-L1 is farnesylated and associated with neuronal membranes, including the endoplasmic reticulum. This modification is not present in UCH-L3, which appears to serve different biochemical and biological roles than UCH-L1 (22–29). The amount of membrane-associated UCH-L1 (UCH-L1^{M}) is linked to intracellular α-synuclein levels and neurotoxicity. We found that chemical inhibition of UCH-L1 farnesylation reduces α-synuclein levels and improves neuronal cell viability in cellular models of α-synuclein-associated toxicity. These results suggest that UCH-L1^{M} plays a role in α-synuclein degradation and PD pathogenesis, and that inhibition of UCH-L1 farnesylation with farnesyl transferase inhibitors (FTIs) has potential as a therapeutic strategy for PD and related synucleinopathies.

Results

A Subpopulation of UCH-L1 (UCH-L1^{M}) Is Tightly Bound to Membranes. UCH-L1 is associated with the plasma membrane of oocytes (2) and with rat brain synaptic vesicles (26). To probe the potential basis for these observations, we studied the membrane-binding characteristics of UCH-L1 in synaptic vesicles isolated from rat brain. Like the integral membrane protein synaptophysin, but unlike synapsin-1 (a peripheral membrane protein), UCH-L1 could not be separated from synaptic vesicles by increasing salt concentration. Treatment with detergent was required to completely solubilize UCH-L1 (Fig. 1*A*), indicating that a portion of UCH-L1 is tightly associated with membranes (designated UCH-L1^{M} below).

When analyzed by 2D gel electrophoresis, the membrane fraction from rat brain lysate contained a single UCH-L1 species that differed from recombinant UCH-L1 (Fig. 1*Bi* compared with *ii*). The unfractionated rat brain homogenate contained both of these species, as well as a third major UCH-L1 species, which may be phosphorylated and/or *O*-glycosylated (Fig. 1*Biii*) (20). These 3 forms of UCH-L1 also were found in cell lysates from human neuroblastoma SH-SY5Y cells (Fig. 1*Biv*). H1299 cells, a non-small cell lung cancer cell line that expresses high levels of UCH-L1, contained a small amount of unmodified

Author contributions: Z.L., R.K.M., R.A.F., M.R.C., and P.T.L. designed research; Z.L., R.K.M., T.N.G., R.A.F., Y.L., and T.L. performed research; Z.L., R.K.M., T.N.G., R.A.F., M.R.C., Y.L., and P.T.L. analyzed data; and R.K.M. and P.T.L. wrote the paper.

The authors declare no conflict of interest.

This article is a PNAS Direct Submission. D.M.H. is a guest editor invited by the Editorial Board.

Freely available online through the PNAS open access option.

[1]To whom correspondence should be addressed. E-mail: peter@linkmedicine.com.

This article contains supporting information online at www.pnas.org/cgi/content/full/0806474106/DCSupplemental.

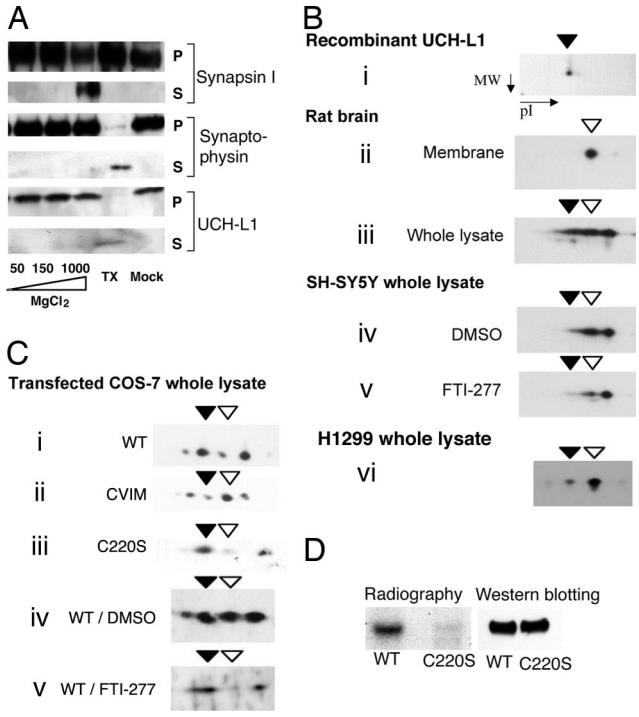

Fig. 1. A portion of UCH-L1 is membrane-associated and farnesylated. (*A*) Rat brain synaptic vesicle fractions were treated with increasing salt concentrations, detergent (TX), or buffer only (Mock), as indicated. Proteins that dissociated from the vesicles were collected in supernatant fractions (S), and those that remained with the vesicular membranes were collected in the pellet fractions (P). The presence of synapsin I, synaptophysin, and UCH-L1 in each fraction was determined by Western blotting. Similar results were obtained with NaCl and KCl salts. (*B*) 2D electrophoresis followed by Western blot analysis using UCH-L1 antibody was performed on recombinant UCH-L1 protein (*i*); on the membrane fraction (*ii*) and whole lysate (*iii*) of rat brain; on lysates of SH-SY5Y cells treated with DMSO (*iv*) or 100 nM FTI-277 (*v*); and on H1299 cell lysate (*vi*). (*C*) Two-dimensional analysis was performed as in *B* on lysates of COS-7 cells transfected with WT (*i*), CVIM (*ii*), or C220S UCH-L1 (*iii*); and on lysates of WT UCH-L1-transfected cells treated with DMSO (*iv*) or 100 nM FTI-277 (*v*). Closed arrowheads indicate forms of UCH-L1 that have the same pI value as the recombinant protein; open arrowheads indicate species corresponding to the form of UCH-L1 found in the membrane fraction. (*D*) COS-7 cells expressing either WT or C220S FLAG-tagged UCH-L1 were radiolabeled with [^{3}H]farnesol and immunoprecipitated by using anti-FLAG antibody. Eluted proteins were analyzed by radiography and by Western blotting for UCH-L1.

UCH-L1, but mostly had the membrane-associated form (Fig. 1*Bvi*). WT UCH-L1-transfected COS-7 cells (which produce low levels of UCH-L1 endogenously), contained 4 UCH-L1 species, 2 of which corresponded to the unmodified and membrane-associated forms (Fig. 1*Ci*)

Membrane-Associated UCH-L1 Is Farnesylated at Cysteine 220. We investigated possible posttranslational modifications that are known to increase membrane binding. Prenylation involves the attachment of a 15-carbon farnesyl or a 20-carbon geranylgeranyl lipid to a cysteine residue in proteins containing a C-terminal CaaX motif (C is cysteine, a is aliphatic, and X is usually serine, methionine, glutamine, alanine, or threonine). UCH-L1 contains an atypical farnesylation sequence at its C terminus (CKAA-CO_2H) that is not present in UCH-L3 (Fig. S1*A*). Sequence analysis suggested that the C terminus of UCH-L1 may support farnesylation but is unlikely to support geranylgeranylation (30). Because direct detection of prenylated proteins by biophysical means is problematic (30, 31), and our own attempts to identify farnesylated UCH-L1 by mass spectrometric analysis were unsuccessful, we used several different approaches to demonstrate farnesylation of UCH-L1. First, to establish that the CKAA sequence serves as a substrate for farnesylation, a fluorescent pentapeptide substrate containing the CKAA sequence was shown to be an in vitro substrate of recombinant mammalian FTase (K_m, ≈70 μM; V_{max}, ≈700 relative fluorescence units per min; Fig. S2*A*), albeit a much weaker one than an analogous peptide substrate containing an optimal CaaX sequence from Ras, CVIM (32) (K_m, ≈3 μM; V_{max}, ≈4,000 relative fluorescence units per min; Fig. S2*B*).

Consistent with the premise that UCH-L1^M is farnesylated, its abundance was demonstrated to be sensitive to the following genetic and chemical perturbations. First, in transfected COS-7 cells subject to 2D analysis, changing the 3 C-terminal amino acids of UCH-L1 from KAA to VIM (K221V/A222I/A223M, or CVIM) increased the abundance of the UCH-L1^M spot (Fig. 1*C*, open arrowheads) relative to the soluble forms of UCH-L1 (Fig. 1*Ci* compared with *ii*). Second, mutation of the putative farnesyl "acceptor" Cys residue of the UCH-L1 CKAA sequence to Ser (C220S) essentially eliminated the membrane-associated species (Fig. 1*Ci* compared with *iii*). The membrane spot in Fig. 1*Ciii* may be due to endogenous UCH-L1 in COS-7 cells. Third, treatment with the commercially available FTase inhibitor FTI-277 (33) decreased the amount of transfected WT UCH-L1^M (Fig. 1*Civ* vs. *v*). Finally, treatment of SH-SY5Y cells with FTI-277 decreased the abundance of endogenous UCH-L1^M (Fig. 1*Biv* compared with *v*). It is important to note that FTI-277 is highly selective for FTase over geranygeranyl transferase (34).

Further evidence that supports UCH-L1^M being farnesylated was obtained from radiolabel incorporation: in transfected COS-7 cells labeled with [^{3}H]farnesol, WT UCH-L1 incorporated the radiolabel, whereas the C220S mutant did not (Fig. 1*D*). In addition, treatment of SH-SY5Y cells with [^{14}C]mevalonic acid or [^{3}H]farnesol resulted in incorporation of the radiolabel into endogenous UCH-L1 (Fig. S1*B*). Finally, UCH-L1 was immunoprecipitated from the membrane fraction of SH-SY5Y cell lysate by using an anti-farnesyl antibody (Fig. S1*C*) (35).

UCH-L1 Is Associated with the Endoplasmic Reticular Membrane. Fluorescence microscopy was used to examine the localization of membrane-associated UCH-L1. COS-7 cells were transiently transfected with either GFP or N-terminally GFP-tagged UCH-L1 and subjected to alcohol fixation, a procedure that removes most cytosolic proteins from cells while retaining most of those that are membrane-bound and/or associated with other membrane-bound proteins (36, 38). Alcohol fixation caused leakage of free GFP from cells, whereas GFP-UCH-L1 was retained (Fig. 2*A*), consistent with the membrane association of UCH-L1^M. Much of GFP-UCH-L1 in these cells was perinuclear, strongly resembled an endoplasmic reticulum (ER) staining pattern, and colocalized with the ER protein calreticulin (Fig. 2*Bi*). Immunostaining of endogenous UCH-L1 in differentiated SH-SY5Y cells and in H1299 cells revealed similar results (Fig. 2*B ii* and *iii*). Although UCH-L1 is reported to interact with Lamp2a (38), we did not observe colocalization with lysosomal markers Lamp1 or Lamp2 (Fig. S3), suggesting that under the conditions of our experiments, UCH-L1^M predominantly localizes to ER membranes. In contrast to cellular fractionation results, we found that the C220S farnesylation site mutation did not affect the overall localization of GFP-UCH-L1 in alcohol-fixed cells. This discrepancy may arise from differences in the extent to which the 2 techniques preserve or disrupt additional (non-farnesylation-based) factors that contribute to the membrane localization of UCH-L1. For example, it is possible that UCH-L1, like some other prenylated proteins (39, 40), may possess weak intrinsic membrane affinity in the absence of farnesylation, and that farnesylation strengthens this interaction. It is also possible that GFP-C220S has affinity for another

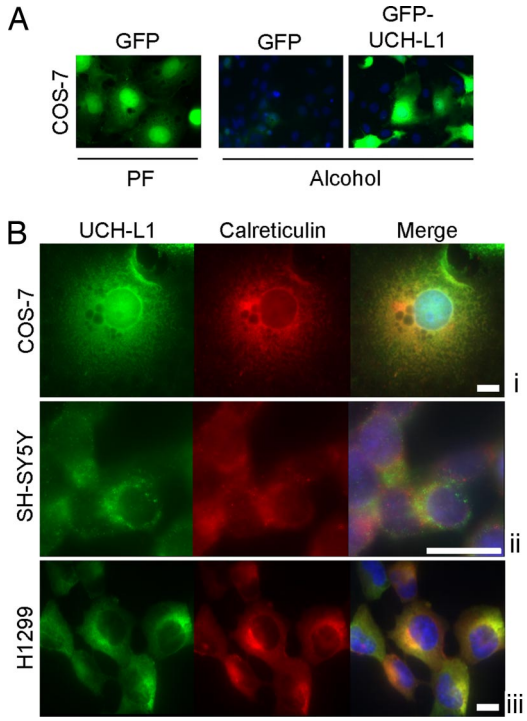

Fig. 2. UCH-L1 associates with the endoplasmic reticular membrane. (*A*) COS-7 cells were transiently transfected with either GFP or GFP-UCH-L1, as indicated. Cells were fixed in paraformaldehyde (PF) or alcohol, and GFP fluorescence was imaged by using identical exposure times and image settings. Alcohol fixation releases cytosolic proteins, including free GFP, from cells. (*B*) Fluorescence microscopy was used to image COS-7 cells transfected with GFP-UCH-L1 and immunostained with calreticulin antibody (*i*), as well as SH-SY5Y (*ii*) and H1299 (*iii*) cells immunostained with UCH-L1 and calreticulin antibodies. COS-7 and SH-SY5Y cells were fixed in alcohol; H1299 cells were fixed in paraformaldehyde. Green indicates UCH-L1; red, calreticulin; yellow, colocalization; and blue, DAPI nuclear stain. (Scale bar: 10 μm.)

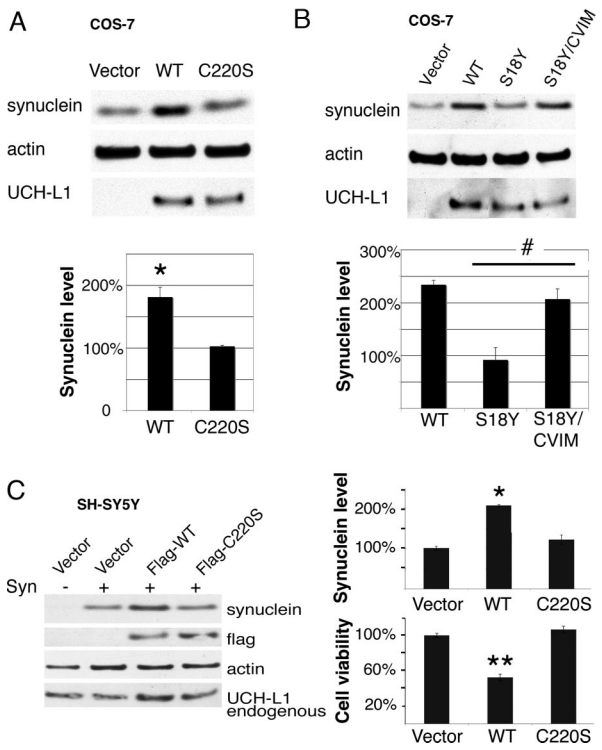

Fig. 3. α-Synuclein accumulation and toxicity are increased by farnesylated UCH-L1. (*A* and *B*) COS-7 cells were transfected with α-synuclein plus either vector or UCH-L1 variants, as indicated. At 72 h later, protein levels were determined by Western blotting of cell lysates and densitometric analysis. α-Synuclein levels were normalized to actin and plotted relative to vector control. (*C*) SH-SY5Y cells were cotransfected with α-synuclein (Syn) and N-terminally Flag-tagged UCH-L1 (WT or C220S), as indicated. Cell lysates were analyzed as above. In parallel, cell viability was assessed by flow cytometry based on cell size, complexity, and membrane integrity. Cell numbers were normalized against control cells transfected with α-synuclein and vector; $n = 3$. Data represent mean $\pm$ SE throughout (#, $P < 0.05$; *, $P < 0.005$; **, $P < 0.001$).

membrane-bound protein, for example, endogenous UCH-L1^{M}. This proposal is consistent with the fact that UCH-L1 forms homodimers in solution (26, 41).

UCH-L1^{M} Comprises ≈30% of Total UCH-L1 in Diseased and Normal Human Brain. UCH-L1^{M} and soluble UCH-L1 (UCH-L1^{S}) were measured in human cortical brain tissue. Ten human brains (5 PD patients, 1 multisystem atrophy, 1 AD, and 3 age-matched healthy controls) were analyzed. UCH-L1^{M} comprised 20–50% of total UCH-L1. In mouse brain regions (cortex, hippocampus, striatum, and midbrain), both UCH-L1^{M} and UCH-L1^{S} were found, and their relative amounts varied over a comparable range (Fig. S4).

UCH-L1^{M} Causes Accumulation of α-Synuclein Without Affecting the Proteasome and Exacerbates α-Synuclein Neurotoxicity. A direct or indirect interaction between UCH-L1 and α-synuclein is indicated by genetic studies of PD susceptibility (42). In synaptic vesicles, UCH-L1 has been shown to associate with α-synuclein (26), a protein whose accumulation plays a key role in PD pathogenesis (43). Furthermore, in COS-7 cells, coexpression of WT UCH-L1, but not the protective S18Y variant, increases levels of transfected α-synuclein by inhibiting its degradation (26). Using this system, we found that COS-7 cells cotransfected with C220S UCH-L1, which is not farnesylated to produce UCH-L1^{M} (see above), do not accumulate α-synuclein (Fig. 3*A*). Conversely, *increasing* the amount of UCH-L1^{M} in the S18Y polymorph by replacing the weak CKAA farnesylation motif with the optimal CVIM motif (S18Y/CVIM UCH-L1) led to significantly increased accumulation of α-synuclein relative to S18Y (Fig. 3*B*). Introducing the same change into the WT UCH-L1 farnesylation motif (CVIM UCH-L1) did not significantly increase synuclein levels in transfected COS-7 cells (Fig. S5*A*), possibly because, beyond a threshold level, excess α-synuclein may be secreted in some cell types (44). In SH-SY5Y neuroblastoma cells, however, transfection with CVIM UCH-L1 significantly increased α-synuclein levels over those produced by WT UCH-L1 (Fig. S5*B*), consistent with the hypothesis that UCH-L1^{M} specifically causes α-synuclein accumulation.

The correlation between the amount of UCH-L1^{M} and the amount of cytosolic α-synuclein in COS-7 cells could, in theory, be due to a general inhibitory effect of UCH-L1^{M} on the proteasomal protein degradation pathway (although the relationship between UCH-L1 and this pathway has been questioned; refs. 7 and 15). However, levels of the model proteasome substrate GFPu (45), the endogenous proteasome substrate IκBα (46), and the molecular chaperone Hsp70 (the expression of which is induced specifically by proteasome inhibition; ref. 47), were all insensitive to cotransfection with UCH-L1, suggesting that the proteasomal pathway is not generally inhibited by UCH-L1^{M} (Fig. S6). Furthermore, by using IκBα as a model substrate, we also confirmed that FTI-277 does not inhibit proteasomal degradation (Fig. S6). The possibility that UCH-L1^{M} is involved in a nonproteasomal protein degradation path-

BIOCHEMISTRY

way, such as chaperone-mediated autophagy and/or macroautophagy (48), remains to be investigated. Vogiatzi *et al.* (49) have reported recently that α-synuclein is degraded by both of these pathways in neuroblastoma cells and in primary neurons. Walters *et al.* (7) have suggested that UCH-L1 is involved in a lysosomal pathway.

To determine whether a neurotoxic form of α-synuclein is specifically increased by UCH-L1^{M}, we tested the effect of UCH-L1 overexpression in the SH-SY5Y human neuroblastoma cell line, which endogenously expresses UCH-L1 and α-synuclein. Overexpression of α-synuclein beyond endogenous levels can be cytotoxic in these cells, depending on the level of overexpression (50). SH-SY5Y cells were cotransfected with WT α-synuclein (≈2-fold increase over endogenous) plus either WT or C220S UCH-L1. As in COS-7 cells, increased accumulation of α-synuclein occurred when WT UCH-L1, but not C220S UCH-L1, was cotransfected. [C220S had in vitro ubiquitin hydrolase activity comparable to the WT protein (Fig. S7.)] Furthermore, a reduction in cell viability occurred in SH-SY5Y cells transfected with α-synuclein plus WT UCH-L1, but not in cells transfected with α-synuclein plus C220S UCH-L1 (Fig. 3*C*). Transfection of either UCH-L1 or α-synuclein alone had no effect on SH-SY5Y viability (Fig. S8). Taken together, these results suggest that UCH-L1^{M} promotes the accumulation and neurotoxicity of α-synuclein in cell culture.

FTI-277 Reduces the Accumulation and Neurotoxicity of α-Synuclein by Inhibiting Farnesylation of UCH-L1. FTI-277 reduced the amount of UCH-L1^{M} in SH-SY5Y cells (see above); subsequent experiments were conducted to determine whether FTI-277 also would reduce the neurotoxicity of α-synuclein. Overexpression of α-synuclein at very high levels by adenoviral infection results in a 20–40% decrease in SH-SY5Y cell viability. Under these conditions, FTI-277 treatment significantly reduced the toxicity (Fig. 4*A*) and the accumulation (Fig. 4*B*) of α-synuclein. Treatment of SH-SY5Y cells with FTI-277 had no effect on endogenous α-synuclein or UCH-L1 transcript levels (Fig. S9), nor did it affect viability of noninfected control cells (Fig. 4*A*). Because FTase inhibition affects protein substrates other than UCH-L1 (51), we sought direct evidence for the involvement of UCH-L1 in producing this effect. Reducing the expression level of endogenous UCH-L1 (by ≈80%) with UCH-L1-specific RNAi eliminated the rescue effect of FTI-277 (Fig. 4*C*). Furthermore, treatment with a UCH-L1 active site-directed inhibitor LDN-57414 (52) also eliminated the rescue effect of FTI-277 (Fig. 4*D*). These results support the hypothesis that decreasing the ratio of farnesylated to nonfarnesylated UCH-L1 by FTI-277 is responsible, at least in part, for its amelioration of α-synuclein neurotoxicity.

The toxicity of α-synuclein toward mouse primary dopaminergic neurons also was reduced by FTI-277. Dopaminergic neurons in mouse midbrain mixed primary cultures are selectively sensitive to virally delivered α-synuclein (53). Transduction with a familial PD-linked variant of α-synuclein (A53T) causes the selective death of tyrosine hydroxylase (TH)-positive (i.e., dopaminergic) neurons (WT α-synuclein could not be expressed at high enough levels to produce toxicity in this system; ref. 53). Treatment of these midbrain cultures with FTI-277 significantly reduced α-synuclein toxicity (Fig. 4*E*). To test the effect of FTI-277 on endogenous α-synuclein, we studied primary cortical neurons, which express α-synuclein at significantly higher levels than SH-SY5Y cells. Treatment with FTI-277 significantly lowered endogenous α-synuclein protein levels in primary cortical neurons (Fig. 4*F*).

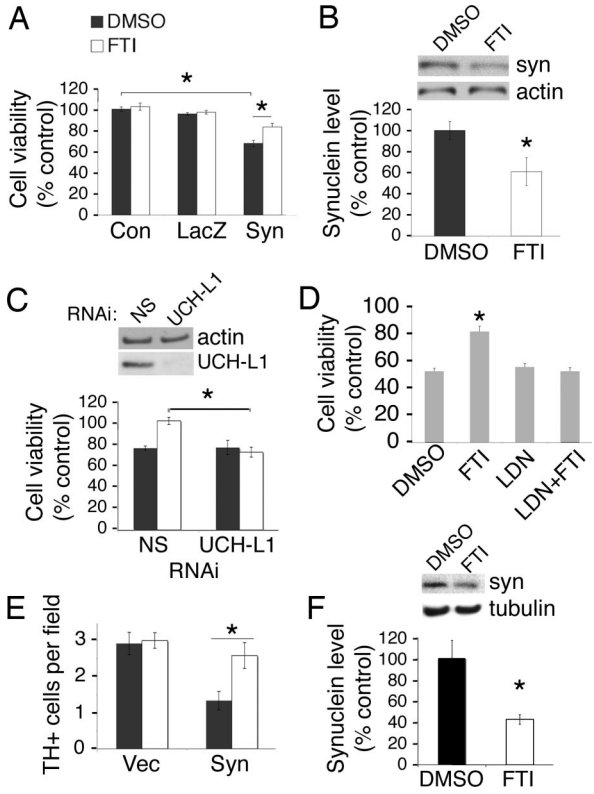

Fig. 4. An FTase inhibitor reduces α-synuclein accumulation and toxicity by a mechanism requiring the expression and activity of UCH-L1. (*A*) Cell viability was measured by MTT assay in SH-SY5Y cells infected with control virus (Con), virus expressing LacZ, or virus expressing α-synuclein (Syn) and treated with either DMSO or 100 nM FTI-277 ($n = 3$; *, $P < 0.05$). Values represent mean ± SE throughout. (*B*) α-Synuclein levels were quantified by Western blotting and normalization to actin in SH-SY5Y cells infected with α-synuclein-expressing virus and treated with either DMSO or 100 nM FTI-277 ($n = 3$; *, $P < 0.05$). (*C*) SH-SY5Y cells were transfected with either nonspecific (NS) or UCH-L1-specific siRNA oligos, followed by infection with α-synuclein-expressing virus and treatment with either DMSO or 100 nM FTI-277. Cell viability was assessed by flow cytometry and normalization against control cells that had undergone the same treatment, except that they were infected with vector instead of α-synuclein. UCH-L1 levels were analyzed by Western blot in a portion of cells before infection ($n = 4$; *, $P < 0.01$). (*D*) SH-SY5Y cells infected with α-synuclein-expressing virus were treated with 100 nM FTI-277, LDN-57414 (LDN), or their combination. Viable cells were counted by trypan blue staining ($n = 3$; *, $P < 0.05$) (*E*) Primary midbrain cultures were infected with either vector (Vec) or α-synuclein-expressing virus (Syn) and treated with DMSO or 100 nM FTI-277. Following treatment, tyrosine hydroxylase-positive (TH+) neurons were counted by using immunofluorescence microscopy. Four fields were counted and averaged in each of 3 independent experiments ($n = 3$; *, $P < 0.01$). (*F*) Endogenous α-synuclein levels were quantified as in *B* in cultured primary cortical neurons treated with either DMSO or 100 nM FTI-277 ($n = 4$; *, $P < 0.05$). Tubulin was used for normalization.

Discussion

UCH-L1 may participate in apoptosis, ubiquitin homeostasis, long-term potentiation (54), chaperone-mediated autophagy (38), and protection against oxidative stress (15), but its role in these processes is not understood. The discovery and characterization of a membrane-associated and farnesylated form of UCH-L1 provide a new target for further investigation of UCH-L1's role in these phenomena. Membrane association of UCH-L1 may be important to facilitate its interaction with other membrane-associated proteins, such as Lamp-2A (38), to promote its oligomerization (26, 28), and/or to induce enzymatic activity (22). Although multiple forms of UCH-L1 have been identified in cell culture and in tissue (16, 55–57), the possibility that one could be farnesylated had not been entertained previously (58). For example, one previous study showed that membrane-associated UCH-L1 is more abundant (and the sol-

uble form less abundant by an equal amount) in the brain of a transgenic mouse model for AD (APP/PS1) (16). A recent study has shown that changes in UCH-L1 mRNA do not correlate with changes in soluble UCH-L1 (7), leaving open the possibility that UCH-L1^{M} is involved.

In addition, the relationship between UCH-L1^{M} and disease must be clarified, because disease-associated decreases in UCH-L1 expression (e.g., in lysosomal storage disorders; ref. 17), may not affect both forms equally. It will also be important for future proteomic investigations to separately quantify all forms of UCH-L1 (18, 59–61). For example, 2 apparently contradictory studies of UCH-L1 abundance in the substantia nigra of PD brain may, in fact, be consistent: one study used quantitative Western blotting to measure soluble UCH-L1 (i.e., UCH-L1^{S}) and showed a decrease of ≈30% in the PD brain (18), whereas another analyzed urea- and detergent-solubilized protein extracts using 2D gel electrophoresis followed by mass spectrometry to show an increase of ≈30% in one UCH-L1 species in the PD brain (59). Our preliminary studies reported here failed to detect an association between the UCH-L1^{M}/UCH-L1^{S} ratio and disease, but a much more extensive study is called for, because the change in ratio required to influence PD susceptibility would be expected to be quite small.

The link between UCH-L1^{M} and accumulation and neurotoxicity of α-synuclein suggests that farnesyl transferase inhibitors that reduce the amount of UCH-L1^{M} may be useful for the treatment of PD and related synucleinopathies. The underlying mechanism of this effect may involve the activation or, more precisely, the disinhibition, of a nonproteasomal pathway for α-synuclein degradation, possibly one capable of handling protein aggregates; for example, chaperone-mediated autophagy or macroautophagy, both of which play a role in α-synuclein degradation (38, 48, 49). Further elucidation of the molecular details of these pathways may allow the identification of novel therapeutic targets for diseases of protein aggregation.

Materials and Methods

Materials. The sources of all reagents can be found in the *SI Experimental Procedures*.

Methods. Additional experimental procedures can be found in the *SI Experimental Procedures*.

α-Synuclein Accumulation Assays in COS-7 Cells. Cells were transfected with 0.2 μg of pcDNA-α-synuclein and 0.2 μg of pcDNA-UCH-L1 variants or vector by using Lipofectamine 2000 (Invitrogen) according to the manufacturer's protocol. Cells were lysed in SDS lysis buffer (50 mM Tris·HCl, 2% SDS, and 1% Nonidet P-40) by boiling for 10 min, followed by Western blot analysis. Densitometry was performed by using the public domain National Institutes of Health Image program (http://rsb.info.nih.gov/nih-image/).

Salt and Detergent Treatment of Synaptic Vesicle Fraction. The synaptic vesicle-containing fractions were prepared as described elsewhere (26), and experiments were carried out as described previously (62). Briefly, synaptic vesicles were incubated for 30 min on ice with various concentrations of $MgCl_2$, 1% Triton X-100, or control buffer without salts and detergent. Treated synaptic vesicles were subjected to centrifugation at 100,000 × *g* for 30 min. Supernatants and pellets were subjected to SDS/PAGE and Western blotting.

Membrane Fractionation. Cells were lysed in 50 mM Tris·HCl supplemented with 1 mM EDTA and protease inhibitor mixture (Sigma) and were homogenized by passing through 26-gauge needles 10 times. The lysate was clarified by spinning at 600 × *g* for 5 min, and supernatant was subjected to ultracentrifugation at 100,000 × *g* for 2 h to separate into membrane and cytosolic fractions. The membrane fraction was washed with buffer (50 mM Tris·HCl, 1 mM EDTA, and 1 M NaCl) and isolated by centrifugation.

Metabolic Labeling. Cells were treated with 10 μM simvastatin for 8 h before being incubated with labeling medium (regular growth medium plus 1 mCi/mL [^{14}C]mevalonate or [^{3}H]farnesol) for 24 h. Cells were lysed in lysis buffer (50 mM Tris·HCl, 1 mM EDTA, 1% Triton X-100, and 150 mM NaCl) in the presence of protease inhibitor cocktail (Sigma). Cell lysate was clarified by centrifugation at 2,000 × *g* for 10 min, followed by overnight incubation with immunoprecipitating antibody. Protein G agarose beads were used to precipitate antibodies, and bound proteins were eluted with SDS/PAGE sample buffer. Eluent was loaded onto 14% Tris-glycine gels, which were fixed and developed by using the fluorographic reagent Amplify (Amersham).

2D Gel Electrophoresis. Cells were lysed in SDS buffer (50 mM Tris·HCl, pH 8.0, and 0.1% SDS) supplemented with protease inhibitor cocktail. Lysates were boiled for 3 min and treated with DNase and RNase. Lysates were precipitated with ice-cold acetone for at least 2 h, and pellets were resuspended in 2D sample buffer (8 M urea, 0.5% CHAPS, 0.2% DTT, 0.5% IPG buffer, and 0.002% bromophenol blue). 2D electrophoresis was carried out with 7-cm pH 4–7 strips according to the manufacturer's protocol (Amersham Life Science). Identification of UCH-L1 protein spots was performed by alignments with internal control proteins (actin present in cell lysate, and recombinant α-synuclein added to samples), which were detected by reprobing of membranes.

Fluorescence Microscopy. Immunostaining and fluorescence microscopy were performed as described (21), with the following modifications: (*i*) alcohol fixation was performed with either 70% ethanol or 100% methanol, ice-cold for 30 min to overnight (results were equivalent using either fixative and did not depend on fixation length); (*ii*) some images were acquired by using a Zeiss Axiovert 200 inverted microscope with 100× objective; and (*iii*) secondary antibodies also included Alexa Fluor 488 and 568 (Invitrogen). SH-SY5Y cells were differentiated with 10 μM retinoic acid for 2–3 days before analysis.

SH-SY5Y Transfections and Cell Counting. A total of 1 × 10^{6} SH-SY5Y cells were transfected with 2 μg of pcDNA-α-synuclein and pcDNA-Flag-UCH-L1 or pcDNA vector by using an Amaxa nucleofactor II machine (program A-023). At 72 h after transfection, cells were harvested and stained with propidium iodide (PI), and cell viability was assessed by standard flow cytometry techniques (63) using standard forward scattering and side scattering profiles, cell complexity, and membrane integrity by negative PI staining. In addition, cells were lysed in SDS lysis buffer and analyzed by Western blotting.

Adenoviral Infection. Viruses were amplified and purified as described (64). SH-SY5Y cells were grown on 100-mm tissue culture-treated dishes and differentiated with 100 nM retinoic acid for 3–5 days before viral infection (adenoviral vector was a gift from Seung-Jae Lee of the Parkinson's Institute, Sunnyvale, CA), with a multiplicity of infection (moi) of 75. The next day, cells were passaged and treated with compounds for 48 h. At 72 h after infection, cell viability was assessed by 3-(4,5-dimethylthiazol-2-yl)-2,5-diphenyl tetrazolium bromide (MTT) assay and trypan blue cell counting.

RNAi. A total of 1 × 10^{6} SH-SY5Y cells were transfected with 2 μg of synthetic siRNA oligo (Dharmco) by using an Amaxa nucleofactor II machine, program A-023. At 72 h later, cells were infected with adenovirus, followed by 48 h of treatment with 100 nM FTI-277, after which live cells were counted by flow cytometry, as described above.

Primary Cell Culture and Viral Transduction. Primary cell cultures were prepared from postnatal mouse midbrain as described previously (53). Primary neurons were transduced with viral particles with mois of 10, and 100 nM FTI-277 was added to the culture at the same time. Counting of dopaminergic neurons was performed as described (53). Four random fields were chosen per slide, and TH^{+} cells were counted manually by a blinded observer, using 3 slides per condition.

Cortical neuron cultures were prepared according to the published procedure (65). Briefly, neurons were isolated from the neocortex of embryonic day 15–17 mice and plated at 200,000 cells/mL in Neurobasal medium plus B27 supplement without antioxidants (Invitrogen). After 5–7 days, plating medium was renewed, 10 μM cytosine β-D-arabino-furanoside hydrochloride was added, and 5% FBS was used for 3–10 days. FTI-277 or DMSO was added to cultures for 48 h. Cells were lysed with lysis buffer (50 mM Tris·HCl, 2 mM EDTA, and 2% SDS) by boiling for 10 min.

ACKNOWLEDGMENTS. We thank James Warsaw and Edward Rudman for their support, financial and otherwise, during the course of this work; and Craig Justman, Valerie Cullen, Berkley Lynch, and Mark Duggan for their input and critical reading of the manuscript. Finally, we acknowledge the helpful suggestions of Daniel Finley, Michael Wolfe, and Hidde Ploegh, all from Harvard Medical School. This work was supported, in part, by a Morris K. Udall Parkinson's Disease Research Center of Excellence Grant from the National

Institutes of Health (NIH)/National Institute of Neurological Disorders and Stroke, and by the Intramural Research Program of the NIH, National Institute on Aging, project number 1 Z01 AG000953. Y.L. was an NIH postdoctoral fellow during the execution of this research.

1. Saigoh K, et al. (1999) Intragenic deletion in the gene encoding ubiquitin carboxy-terminal hydrolase in gad mice. *Nat Genet* 23:47–51.
2. Sekiguchi S, et al. (2006) Localization of ubiquitin C-terminal hydrolase L1 in mouse ova and its function in the plasma membrane to block polyspermy. *Am J Pathol* 169:1722–1729.
3. Hibi K, et al. (1999) PGP9.5 as a candidate tumor marker for non-small-cell lung cancer. *Am J Pathol* 155:711–715.
4. Takase T, et al. (2003) PGP9.5 overexpression in esophageal squamous cell carcinoma. *Hepatogastroenterology* 50:1278–1280.
5. Yamazaki T, et al. (2002) PGP9.5 as a marker for invasive colorectal cancer. *Clin Cancer Res* 8:192–195.
6. Doran JF, Jackson P, Kynoch PA, Thompson RJ (1983) Isolation of PGP 9.5, a new human neurone-specific protein detected by high-resolution two-dimensional electrophoresis. *J Neurochem* 40:1542–1547.
7. Walters BJ, et al. (2008) Differential effects of Usp14 and Uch-L1 on the ubiquitin proteasome system and synaptic activity. *Mol Cell Neurosci* 39:539–548.
8. Momose Y, et al. (2002) Association studies of multiple candidate genes for Parkinson's disease using single nucleotide polymorphisms. *Ann Neurol* 51:133–136.
9. Maraganore DM, et al. (1999) Case-control study of the ubiquitin carboxy-terminal hydrolase L1 gene in Parkinson's disease. *Neurology* 53:1858–1860.
10. Maraganore DM, et al. (2004) UCHL1 is a Parkinson's disease susceptibility gene. *Ann Neurol* 55:512–521.
11. Wintermeyer P, et al. (2000) Mutation analysis and association studies of the UCHL1 gene in German Parkinson's disease patients. *NeuroReport* 11:2079–2082.
12. Elbaz A, et al. (2003) S18Y polymorphism in the UCH-L1 gene and Parkinson's disease: Evidence for an age-dependent relationship. *Mov Disord* 18:130–137.
13. Xue S, Jia J (2006) Genetic association between ubiquitin carboxy-terminal hydrolase-L1 gene S18Y polymorphism and sporadic Alzheimer's disease in a Chinese Han population. *Brain Res* 1087:28–32.
14. Naze P, Vuillaume I, Destee A, Pasquier F, Sablonniere B (2002) Mutation analysis and association studies of the ubiquitin carboxy-terminal hydrolase L1 gene in Huntington's disease. *Neurosci Lett* 328:1–4.
15. Kyratzi E, Pavlaki M, Stefanis L (2008) The S18Y polymorphic variant of UCH-L1 confers an antioxidant function to neuronal cells. *Hum Mol Genet* 17:2160–2171.
16. Gong B, et al. (2006) Ubiquitin hydrolase Uch-L1 rescues beta-amyloid-induced decreases in synaptic function and contextual memory. *Cell* 126:775–788.
17. Bifsha P, et al. (2007) Altered gene expression in cells from patients with lysosomal storage disorders suggests impairment of the ubiquitin pathway. *Cell Death Differ* 14:511–523.
18. Barrachina M, et al. (2006) Reduced ubiquitin C-terminal hydrolase-1 expression levels in dementia with Lewy bodies. *Neurobiol Dis* 22:265–273.
19. Larsen CN, Krantz BA, Wilkinson KD (1998) Substrate specificity of deubiquitinating enzymes: Ubiquitin C-terminal hydrolases. *Biochemistry* 37:3358–3368.
20. Cole RN, Hart GW (2001) Cytosolic O-glycosylation is abundant in nerve terminals. *J Neurochem* 79:1080–1089.
21. Meray RK, Lansbury PT, Jr (2007) Reversible monoubiquitination regulates the Parkinson disease-associated ubiquitin hydrolase UCH-L1. *J Biol Chem* 282:10567–10575.
22. Das C, et al. (2006) Structural basis for conformational plasticity of the Parkinson's disease-associated ubiquitin hydrolase UCH-L1. *Proc Natl Acad Sci USA* 103:4675–4680.
23. Harada T, et al. (2004) Role of ubiquitin carboxy terminal hydrolase-L1 in neural cell apoptosis induced by ischemic retinal injury in vivo. *Am J Pathol* 164:59–64.
24. Kwon J, et al. (2006) The region-specific functions of two ubiquitin C-terminal hydrolase isozymes along the epididymis. *Exp Anim* 55:35–43.
25. Kwon J, et al. (2004) Two closely related ubiquitin C-terminal hydrolase isozymes function as reciprocal modulators of germ cell apoptosis in cryptorchid testis. *Am J Pathol* 165:1367–1374.
26. Liu Y, *et al.* (2002) The UCH-L1 gene encodes two opposing enzymatic activities that affect alpha-synuclein degradation and Parkinson's disease susceptibility. *Cell* 111:209–218.
27. Luchansky SJ, Lansbury PT, Jr, Stein RL (2006) Substrate recognition and catalysis by UCH-L1. *Biochemistry* 45:14717–14725.
28. Naito S, et al. (2006) Characterization of multimetric variants of ubiquitin carboxyl-terminal hydrolase L1 in water by small-angle neutron scattering. *Biochem Biophys Res Commun* 339:717–725.
29. Wang YL, et al. (2006) Overexpression of ubiquitin carboxyl-terminal hydrolase L1 arrests spermatogenesis in transgenic mice. *Mol Reprod Dev* 73:40–49.
30. Benetka W, Koranda M, Maurer-Stroh S, Pittner F, Eisenhaber F (2006) Farnesylation or geranylgeranylation? Efficient assays for testing protein prenylation in vitro and in vivo. *BMC Biochem* 7:6.
31. Maurer-Stroh S, et al. (2007) Towards complete sets of farnesylated and geranylgeranylated proteins. *PLoS Comput Biol* 3:e66.
32. Brown MS, *et al.* (1992) Tetrapeptide inhibitors of protein farnesyltransferase: Amino-terminal substitution in phenylalanine-containing tetrapeptides restores farnesylation. *Proc Natl Acad Sci USA* 89s:8313–8316.
33. Sun J, Qian Y, Hamilton AD, Sebti SM (1995) Ras CAAX peptidomimetic FTI 276 selectively blocks tumor growth in nude mice of a human lung carcinoma with K-Ras mutation and p53 deletion. *Cancer Res* 55(19):4243–4247.
34. Lerner EC, et al. (1995) Ras CAAX peptidomimetic FTI-277 selectively blocks oncogenic Ras signaling by inducing cytoplasmic accumulation of inactive Ras-Raf complexes. *J Biol Chem* 270:26802–26806.
35. Baron R, et al. (2000) RhoB prenylation is driven by the three carboxyl-terminal amino acids of the protein: Evidenced in vivo by an anti-farnesyl cysteine antibody. *Proc Natl Acad Sci USA* 97:11626–11631.
36. Jiang W, Hunter T (1998) Analysis of cell-cycle profiles in transfected cells using a membrane-targeted GFP. *Biotechniques* 24:349–350, 352, 354.
37. Kalejta RF, Shenk T, Beavis AJ (1997) Use of a membrane-localized green fluorescent protein allows simultaneous identification of transfected cells and cell cycle analysis by flow cytometry. *Cytometry* 29:286–291.
38. Kabuta T, Furuta A, Aoki S, Furuta K, Wada K (2008) Aberrant interaction between Parkinson's disease-associated mutant UCH-L1 and the lysosomal receptor for chaperone-mediated autophagy. *J Biol Chem* 283:23731–23738.
39. Kouno T, et al. (2005) Solution structure of microtubule-associated protein light chain 3 and identification of its functional subdomains. *J Biol Chem* 280:24610–24617.
40. Liu L, et al. (1995) Synthetic prenylated peptides: Studying prenyl protein-specific endoprotease and other aspects of protein prenylation. *Methods Enzymol* 250:189–206.
41. Nishikawa K, et al. (2003) Alterations of structure and hydrolase activity of parkinsonism-associated human ubiquitin carboxyl-terminal hydrolase L1 variants. *Biochem Biophys Res Commun* 304:176–183.
42. Maraganore DM, et al. (2003) Complex interactions in Parkinson's disease: A two-phased approach. *Mov Disord* 18:631–636.
43. Goldberg MS, Lansbury PT, Jr (2000) Is there a cause-and-effect relationship between alpha-synuclein fibrillization and Parkinson's disease? *Nat Cell Biol* 2:E115–E119.
44. Lee SJ (2008) Origins and effects of extracellular alpha-synuclein: Implications in Parkinson's disease. *J Mol Neurosci* 34:17–22.
45. Bence NF, Sampat RM, Kopito RR (2001) Impairment of the ubiquitin-proteasome system by protein aggregation. *Science* 292:1552–1555.
46. Palombella VJ, Rando OJ, Goldberg AL, Maniatis T (1994) The ubiquitin-proteasome pathway is required for processing the NF-kappa B1 precursor protein and the activation of NF-kappa B. *Cell* 78:773–785.
47. Bush KT, Goldberg AL, Nigam SK (1997) Proteasome inhibition leads to a heat-shock response, induction of endoplasmic reticulum chaperones, and thermotolerance. *J Biol Chem* 272:9086–9092.
48. Pan T, Kondo S, Le W, Jankovic J (2008) The role of autophagy-lysosome pathway in neurodegeneration associated with Parkinson's disease. *Brain* 131:1969–1978.
49. Vogiatzi T, Xilouri M, Vekrellis K, Stefanis L (2008) Wild type a-synuclein is degraded by chaperone mediated autophagy and macroautophagy in neuronal cells. *J Biol Chem* 283:23542–23556.
50. Oluwatosin-Chigbu Y, et al. (2003) Parkin suppresses wild-type alpha-synuclein-induced toxicity in SHSY-5Y cells. *Biochem Biophys Res Commun* 309:679–684.
51. Wright LP, Philips MR (2006) Thematic review series: Lipid posttranslational modifications. CAAX modification and membrane targeting of Ras. *J Lipid Res* 47:883–891.
52. Liu Y, et al. (2003) Discovery of inhibitors that elucidate the role of UCH-L1 activity in the H1299 lung cancer cell line. *Chem Biol* 10:837–846.
53. Petrucelli L, et al. (2002) Parkin protects against the toxicity associated with mutant alpha-synuclein: Proteasome dysfunction selectively affects catecholaminergic neurons. *Neuron* 36:1007–1019.
54. Setsuie R, Wada K (2007) The functions of UCH-L1 and its relation to neurodegenerative diseases. *Neurochem Int* 51:105–111.
55. DiPaolo BR, Pignolo RJ, Cristofalo VJ (1995) Identification of proteins differentially expressed in quiescent and proliferatively senescent fibroblast cultures. *Exp Cell Res* 220:178–185.
56. Farooqui SM (1994) Induction of adenylate cyclase sensitive dopamine D2-receptors in retinoic acid induced differentiated human neuroblastoma SHSY-5Y cells. *Life Sci* 55:1887–1893.
57. Kawakami T, et al. (1999) Isolation and characterization of cytosolic and membrane-bound deubiquitinylating enzymes from bovine brain. *J Biochem* 126:612–623.
58. McTaggart SJ (2006) Isoprenylated proteins. *Cell Mol Life Sci* 63:255–267.
59. Basso M, et al. (2004) Proteome analysis of human substantia nigra in Parkinson's disease. *Proteomics* 4:3943–3952.
60. Choi J, et al. (2004) Oxidative modifications and down-regulation of ubiquitin carboxyl-terminal hydrolase L1 associated with idiopathic Parkinson's and Alzheimer's diseases. *J Biol Chem* 279:13256–13264.
61. Schweitzer K, et al. (2006) Aberrantly regulated proteins in frontotemporal dementia. *Biochem Biophys Res Commun* 348:465–472.
62. Kubo SI, et al. (2001) Parkin is associated with cellular vesicles. *J Neurochem* 78:42–54.
63. Otsuki Y, Li Z, Shibata MA (2003) Apoptotic detection methods–from morphology to gene. *Prog Histochem Cytochem* 38:275–339.
64. Gosavi N, Lee HJ, Lee JS, Patel S, Lee SJ (2002) Golgi fragmentation occurs in the cells with prefibrillar alpha-synuclein aggregates and precedes the formation of fibrillar inclusion. *J Biol Chem* 277:48984–48992.
65. Hartley DM, et al. (1999) Protofibrillar intermediates of amyloid beta-protein induce acute electrophysiological changes and progressive neurotoxicity in cortical neurons. *J Neurosci* 19:8876–8884.